Monomeric, Base-Free Mn(II) Dialkyls; Synthesis, Magnetic Properties and Molecular Structure of MnR_2 [R = $CH(SiMe_3)_2$], SCF MO Calculations on $Mn(CH_3)_2$ and Photoelectron Spectra of $Mn(CH_2CMe_3)_2$

Richard A. Andersen,[a] David J. Berg,[a] Liv Fernholt,[b] Knut Fægri, Jr.,[b] Jennifer C. Green,[c] Arne Haaland,[b] Michael F. Lappert,[d] Wing-Por Leung[d] and Kristian Rypdal[b]

[a]Department of Chemistry, University of California, Berkeley, California 94720, U.S.A., [b]Department of Chemistry, University of Oslo. P.O. Box 1033, Blindern, N-0315 Oslo 3, Norway, [c]Inorganic Chemistry Laboratories, South Parks Road, Oxford OX1 3QR and [d]School of Chemistry and Molecular Sciences, University of Sussex, Brighton, BN1 9QJ, UK

Andersen, R. A., Berg, D. J., Fernholt, L., Fægri, K., Jr., Green, J. C., Haaland, A., Lappert, M. F., Leung, W.-P. and Rypdal, K., 1988. Monomeric, Base-Free Mn(II) Dialkyls; Synthesis, Magnetic Properties and Molecular Structure of MnR_2 [R = $CH(SiMe_3)_2$], SCF MO Calculations on $Mn(CH_3)_2$ and Photoelectron Spectra of $Mn(CH_2CMe_3)_2$. – Acta Chem. Scand., Ser. A 42: 554–562.

MnR_2 [R = $CH(SiMe_3)_2$] has been prepared from $MnCl_2$ and LiR in diethyl ether. The compound is monomeric in pentane and in the gas phase. The magnetic susceptibility from 5 to 240 K follows the Curie-Weiss law with μ_{eff} = 5.49 B.M., indicating the presence of monomeric *high-spin* species. Gas electron diffraction data are consistent with ∠CMnC = 180° and Mn–C = 201(3) pm. The mean Si–C bond distance, 186.9(2) pm, is significantly smaller, and the valence angle <SiCSi = 130(2)° significantly larger than in $H_2C(SiMe_3)_2$ or in the main group metal analogues GeR_2 and SnR_2. SCF MO calculations on *high-spin* $^6A_1'$ $Mn(CH_3)_2$ yields an optimal bond distance of 213 pm and indicates that the net charge on Mn is +1.40. The photoelectron spectrum of $Mn(CH_2CMe_3)_2$ has been recorded and assigned.

Dedicated to Professor Otto Bastiansen on his 70th birthday

The first homoleptic manganese(II) alkyls appear to have been synthesized by Wilkinson and coworkers.[1] X-Ray diffraction studies have shown that $Mn(CH_2SiMe_3)_2$ forms a linear alkyl-bridged polymer (like that of $BeMe_2$[2]) in the solid phase, $Mn(CH_2CMe_3)_2$ forms a linear tetramer, and $Mn(CH_2CMe_2Ph)_2$ a dimer.[1] Dimesitylmanganese forms a linear trimer in the crystalline phase,[3] while $Mn\{C(SiMe_3)_3\}_2$ is monomeric with ∠CMnC = 180° and the bond distance Mn–C = 210.2(4) pm.[4]

The gas electron diffraction pattern of $Mn(CH_2CMe_3)_2$ (= $Mnnp_2$) recorded with a nozzle temperature of ca. 140 °C showed that under the experimental conditions the gas was monomeric, and yielded the bond distance Mn–C = 210.4(6) pm.[5]

$Mn\{C(SiMe_3)_3\}_2$ has a magnetic moment of ca. 5.1 B.M. (determined by the Evans[6] method),[4] and is thus predominantly if not exclusively *high-spin*, $S = 5/2$. The ESR spectra of $Mn(CH_2CMe_2Ph)_2$, $Mnnp_2$, and $Mn(CH_2SiMe_3)_2$ in hydrocarbon solvents were consistent with the presence of oligomeric species with antiferromagnetic coupling between *high-spin* Mn centers.[1]

In this article we describe (i) the synthesis and characterization of $Mn\{CH(SiMe_3)_2\}_2$ (= MnR_2), (ii) the magnetic susceptibility of MnR_2 measured from 5 to 240 K, (iii) the molecular structure of MnR_2 determined by gas electron diffraction, (iv)

the results of *ab initio* molecular orbital calculations on *high-spin* $MnMe_2$, and (v) the photoelectron spectrum of $Mnnp_2$.

Experimental

Synthesis. All manipulations were performed in an inert atmosphere using conventional Schlenk techniques or a dry-box.

A solution of $LiCH(SiMe_3)_2$[7] (1.08 g, 6.5 mmol) in diethyl ether (50 cm^3) was added to a stirred suspension of $MnCl_2$ (0.45 g, 3.6 mmol) in diethyl ether (20 cm^3) at ca. 20 °C. The pink suspension was stirred for ca. 18 h at ca. 20 °C. After removal of volatile material from the filtrate, distillation furnished the pale yellow liquid $Mn\{CH(SiMe_3)_2\}_2$ (= MnR_2), b.p. 100–110 °C/0.5 Torr; m.p. 8–10 °C; mass spectrum (*m/z*, *z* = 1) [assignment]: 373 $[P]^+$, 358 $[P–Me]^+$, 273, 230, 213, 73.

The molecular weight in pentane solution determined by Signers method (essentially ebullioscopy) indicated monomeric species.

Gas electron diffraction. The electron diffraction data for MnR_2 were recorded on a Balzers Eldigraph KDG-2 with reservoir and nozzle temperatures of ca. 120 °C, corresponding to a vapor pressure of about 1 Torr. Exposures were made with nozzle-to-plate distances of 50 and 25 cm. Two plates from the first set and three from the last were subjected twice to photometry, and the optical densities processed by standard procedures. The molecular intensity curves obtained for each distance were averaged and scaled, but

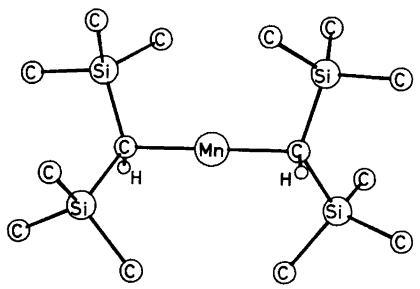

Fig. 1. Molecular model of $Mn\{CH(SiMe_3)\}_2$ (= MnR_2). The model has a two-fold symmetry axis in the plane of the paper and perpendicular to the linear CMnC fragment. Methyl hydrogen atoms have been omitted for clarity.

Table 1. Interatomic distances, r.m.s. vibrational amplitudes (*l*) and valence angles of MnR_2 [R = $CH(SiMe_3)_2$]. Estimated standard deviations in parentheses in units of the last digit. Non-refined parameters are listed in square brackets. C^i = *inner* (methine) C; C^o = *outer* (methyl) C.

	r_a/pm	*l*/pm
Bond distances		
Mn–C^i	201(3)	10(4)
Si–C(mean)	186.9(2)	
Si–C^i	187(3)	6.3(4)[a]
Si–C^o	187(3)	6.3(4)[a]
C–H(mean)	109.5(5)	6.1(6)
Non-bonded distances within $SiMe_3$ group		
C^o···C^o	306(2)	12(2)[b]
Si···H	246(1)	13(2)
Within R = $CH(SiMe_3)_2$ ligand		
Si···Si	339(4)	14(2)[c]
C^i···C^o	305(2)	12(2)[b]
Si···C^o	396(5)	28(10)[d]
Si···C^o	411(4)	28(10)[d]
Si···C^o	488(3)	24(10)[d]
Distances involving Mn and interligand distances		
Mn···Si	318(2)	14(2)[c]
Mn···C^o	333(5)	29(15)[e]
Mn···C^o	350(5)	29(15)[e]
Mn···C^o	387(4)	16(2)[f]
Mn···C^o	410(4)	16(2)[f]
Mn···C^o	475(2)	10(2)[f]
Mn···C^o	482(2)	10(2)[f]
Si···Si	535(8)	16(7)[g]
Si···Si	580(12)	26(7)[g]
Si···Si	617(8)	21(7)[g]
Valence angles/°		
$\angle C^iMnC^i$	[180]	
$\angle MnC^iSi$	110.3(10)	
$\angle MnC^iH$	[106]	
$\angle C^iSiC^o$	110(2)	
$\angle SiC^iSi$	130(2)	
$\angle SiC^oH$	109.3(8)	
Torsion angles/°		
$\Phi[H^iC^i(Mn)C^iH^i]$	128(1)	
$\Phi(SiC^iSiC^o)$	52(2)	
$\Phi(C^iSiC^oH)$	[60]	

[a–g] Indicates groups of amplitudes refined with constant differences.

not connected. The curves extended from s = 15.00 to 145.00 nm^{-1} with increment ΔS = 1.25 nm^{-1}, and from s = 25.00 to 285.00 nm^{-1} with increment 2.50 nm^{-1}.

Atomic scattering factors, $f'(s)$, were taken from Schäfer *et al.*[8] The molecular intensities were modified through multiplication with $s/|f'_{Mn}||f'_{C}|$.

Structure refinement. Structure refinements by least-squares calculations on the intensity data were based on a molecular model of C_2 symmetry as indicated in Fig. 1. In addition it was assumed that:

(i) $\angle C^iMnC^i = 180°$. (C^i = *inner* – or methine – C atom);
(ii) each MnC^iHSi_2 fragment has C_s symmetry. $\angle MnC^iH$ was fixed at 106°;
(iii) each $C^iSi(C^oH_3)_3$ fragment has C_3symmetry. (C^o = *outer* – or methyl – C atom);
(iv) each SiC^oH_3 fragment has C_3 symmetry. C^i-H and C^o-H bond distances were assumed equal; and
(v) each $C^i(SiMe_3)_2$ fragment has C_2 symmetry.

After these assumptions have been made, the molecular structure is determined by ten independent parameters, the Mn-C^i, C^i-Si, Si–C^o and C-H bond distances, the valence angles $\angle MnC^iSi$, $\angle SiC^iSi$, $\angle C^iSiC^o$ and $\angle SiC^oH$, and the dihedral angles $\Phi[H^iC^i(Mn)C^iH^i]$, $\Phi(SiC^iSiC^o)$ and $\Phi(C^iSiC^oH)$. The last refined to values not significantly different from 60° (staggered methyl groups) and was fixed at this value in the final refinements.

The nine remaining parameters and eleven root-mean-square amplitudes of vibration (l) were refined under the constraints of a geometrically consistent r_a model. The best values obtained are listed in Table 1. The quoted e.s.d.'s have been multiplied by a factor of 3.0 to compensate for uncertainty due to data correlation and unrefined parameters. An experimental radial distribution curve and a difference curve is shown in Fig. 2.

Magnetic susceptibility studies. Magnetic susceptibility measurements were made using a S.H.E. model 905 superconducting magnetometer (SQUID). Liquid MnR_2 was pipetted into one

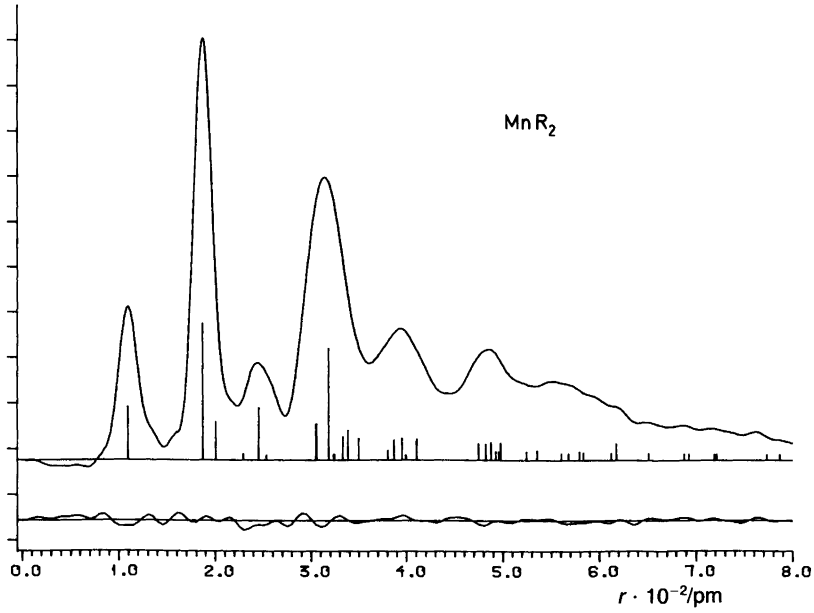

Fig. 2. Experimental radial distribution curve and difference curves for MnR_2. Artificial damping constant k = 20 pm^2. Major interatomic distances are indicated by perpendicular bars.

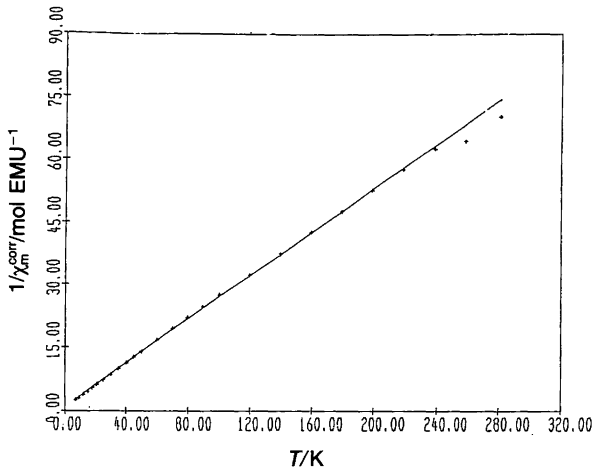

Fig. 3. $1/\chi_m^{corr}$ for MnR_2 as a function of T at 40 kGauss.

half of a threaded KEL-F container in an argon dry-box.

Magnetic susceptibilities were measured at 5 and 40 KG and from 5 to 280 K. The temperature intervals were 3 K from 6 to 21 K, 5 K from 25 to 50 K, 10 K from 50 to 100 K, and 20 K from 100 to 240 K. Instrument problems gave rise to erratic behaviour above 240 K, but this was in no way related to the sample. Molar susceptibilities, χ_M, were corrected for container and sample diamagnetism. A plot of χ_M^{corr} against T is shown in Fig. 3.

Observed $1/\chi_M^{corr}$ values were fitted to

$$1/\chi_M^{corr} = (T-\theta)/C$$

using a program written by Dr. E. Gamp, and effective magnetic moments calculated as $\mu = 2.828\ C^{1/2}$.

The resulting values were $\mu = 5.45$ B.M. and $\theta = -1$ K (at 5 KG), and $\mu = 5.53$ B.M. and $\theta = -3$ K (at 40 KG).

Table 2. Ionization energies for $Mn(CH_2CMe_3)_2$.

Band	I.E./eV	Assignment
A	7.2	Mn 3dσ
B	7.9	σ_u(Mn–C)
C	9.6	σ_g(Mn–C)
D	11.2	ligand
E	12.5	–"–
F	15.2	–"–
G	17.6	–"–
H	21.8	–"–

Photoelectron spectra. Bis*neo*pentylmanganese = $Mnnp_2$ was synthesized as described by Wilkinson and coworkers.[1]

Table 3. Total energies, orbital energies and population parameters obtained by SCF MO calculations on *high-spin* ($^6A_1'$) $Mn(CH_3)_2$.

R(Mn–C)/ pm		Total energy/a.u.
210		−1228.6314
213		−1228.6318
216		−1228.6313
R_e = 213 pm		
Orbital energies for R = 2.10 Å		
		ε/eV
$^5a_2''$	σ(Mn-C)	−8.48
$^7a_1'$	σ(Mn−C)	−10.73
$^4e'$	σ(C–H)	−13.65
$^2e''$	σ(C–H)	−13.71
$^6a_1'$	Mn(dσ)	−14.62
$^1e''$	Mn(dπ)	−16.29
$^3e'$	Mn(dδ)	−16.70
Atomic orbital populations		
Mn	(4s)	0.63
Mn	(dδ)	1.00
Mn	(dπ)	1.00
Mn	(dσ)	1.11
Net charges		
Mn	+1.40	
C	−1.19	
H	+0.16	

He I and He II photoelectron spectra were determined using a PES Laboratories 0078 PE spectrometer interfaced with a Research Machines 380 Z microprocessor. The compound was held at temperatures between 75 and 90 °C during data aquisition. The spectrum was calibrated using N_2, Xe and He.

Molecular orbital calculations. Ab initio molecular orbital calculations on *high-spin* $^6A_1$ Mn $(CH_3)_2$ were carried out with the program DISCO[9] with Gaussian-type basis. For Mn we used a (12*s*, 6*p*, 4*d*) basis[10] contracted to <9*s*, 4*p*, 3*d*>, for C a (7*s*, 3*p*) basis[11] contracted to <4*s*, 2*p*>, and for H a (3*s*) basis[12] contracted to <2*s*>.

Calculations were carried out on a model of D_{3h} symmetry, i.e. with ∠CMnC = 180° and eclipsed methyl groups. The C–H bond distance was fixed at 109 pm, the angle ∠MnCH at 109.5°, and calculations carried out with Mn–C bond distances of 120, 213 and 216 pm. The resulting energies are listed in Table 3. Interpolation yields an optimal Mn–C distance of 213 pm.

Results and discussion

Alkylation of $MnCl_2$ with $(LiR)_n$ [R = CH $(SiMe_3)_2$[7]] in diethyl ether followed by vacuum distillation yields solvent-free MnR_2, m.p. 8–10 °C. The molecular weight in pentane (*M* = 364) was consistent with monomeric species (*M* = 373). The magnetic moment in C_6D_6 solution at ca. 30 °C measured by Evans' method[6] was μ_{eff} = 5.27 B.M.

The magnetic susceptibility of liquid MnR_2 showed Curie-Weiss behaviour from 5 to 240 K with an average magnetic moment of 5.49 B.M. This result demonstrates that the Mn centers are *high-spin*, *S* = 5/2, and magnetically independent, which in turn indicates that the liquid (glass) consists of monomeric species.

$Mn(CH_2SiMe_3)_2$, where each C_α carries one $SiMe_3$ group, forms a linear alkyl-bridge polymer in the solid state.[1] The magnetic moment in benzene solution at ambient temperature (ca. 3.0 B.M.) and ESR spectra in frozen toluene indicated the presence of dimeric (or oligomeric) species with antiferromagnetic coupling between *high-spin* Mn centers.

Variable temperature (5–280 K) magnetic susceptibility studies have been completed for solid $Mn(CH_2SiMe_3)_2$ and show that the compound does not follow Curie-Weiss behaviour, consistent with spin-pairing as a function of temperature. The effective moment of 2.38 B.M. at 282 K and at 5 gauss is consistent with the solution moment. These studies will be reported later.

$Mn\{C(SiMe_3)_3\}_2$, where each C_α carries three $SiMe_3$ groups, is monomeric in the solid phase and in solution;[4] association is presumably prevented by the extreme bulk of the ligand. Our results indicate that two $SiMe_3$ groups attached to each C_α in MnR_2 are sufficient to prevent association.

The gas electron diffraction pattern of MnR_2 was recorded with a nozzle temperature of ca. 120 °C. Least-squares refinement of nine structure parameters and eleven root-mean-square amplitudes of vibration yielded the values listed in Table 1.

The Mn–C bond distance in MnR_2 is 201(3) pm and thus significantly shorter than the Mn–C bond distances in $Mn\{C(SiMe_3)_3\}_2$, viz. 210.2(4) pm,[4] and Mn*np*$_2$, 210.4(6) pm.[5] Inspection of the RD curve for MnR_2 (Fig. 2) shows that the peak representing the two Mn–C bond distances forms a barely perceptible shoulder on the high-*r* side of the much larger peak representing sixteen Si–C distances. Under such circumstances it is difficult to assess not only the best value for Mn–C but also the proper error limits. However, after having made several unsuccessful attempts to obtain satisfactory agreement with a model of MnR_2 with Mn–C near 210 pm, we are confident that the above mentioned difference is real.

The molecular structures of HR [= $H_2C(SiMe_3)_2$] and of the two main group metal dialkyls GeR_2 and SnR_2 have recently been determined by gas electron diffraction.[13,14] Comparison shows that the replacement of an inner, methylene H atom in HR with a *high-spin* Mn(II) atom leads to a significant increase of the ∠SiC^{i}Si angle, from 123.2(9)° to 130(2)° and a slight but significant decrease in the *mean* Si–C bond distance, from 187.8(1) pm to 186.9(2) pm.‡ Both

‡ The two Si–C bond distances Si–C^i and Si–C^o are strongly correlated and cannot be determined with sufficient accuracy to allow the determination of the H to Mn substitution effect on each. It seems probable that the major effect would be on the Si–C^i bonds; if the Si–C^o bonds are assumed unaltered, the observed decrease of the *mean* Si–C bond distance indicates that Si–C^i distances decrease by 4 pm on Mn substitution.

changes are in the opposite direction to those expected from steric considerations, and found in GeR_2 and SnR_2: $\angle SiC^iSi$ = 113.0(5)° (Ge) and 114.0(3)° (Sn) and mean Si–C = 188.5(3) pm (Ge) and 188.6(3) pm (Sn).

These differences prompted us to look for agostic Mn···H interactions[15] in MnR_2. This molecule is too large to allow determination of the position of individual H atoms; only a mean C–H bond distance and a mean $SiC^{\alpha}H$ angle have been refined ; the H atoms are essentially in calculated positions. All Mn to methyl H atom distances are, however, greater than 290 pm, long enough to rule out any significant interactions.

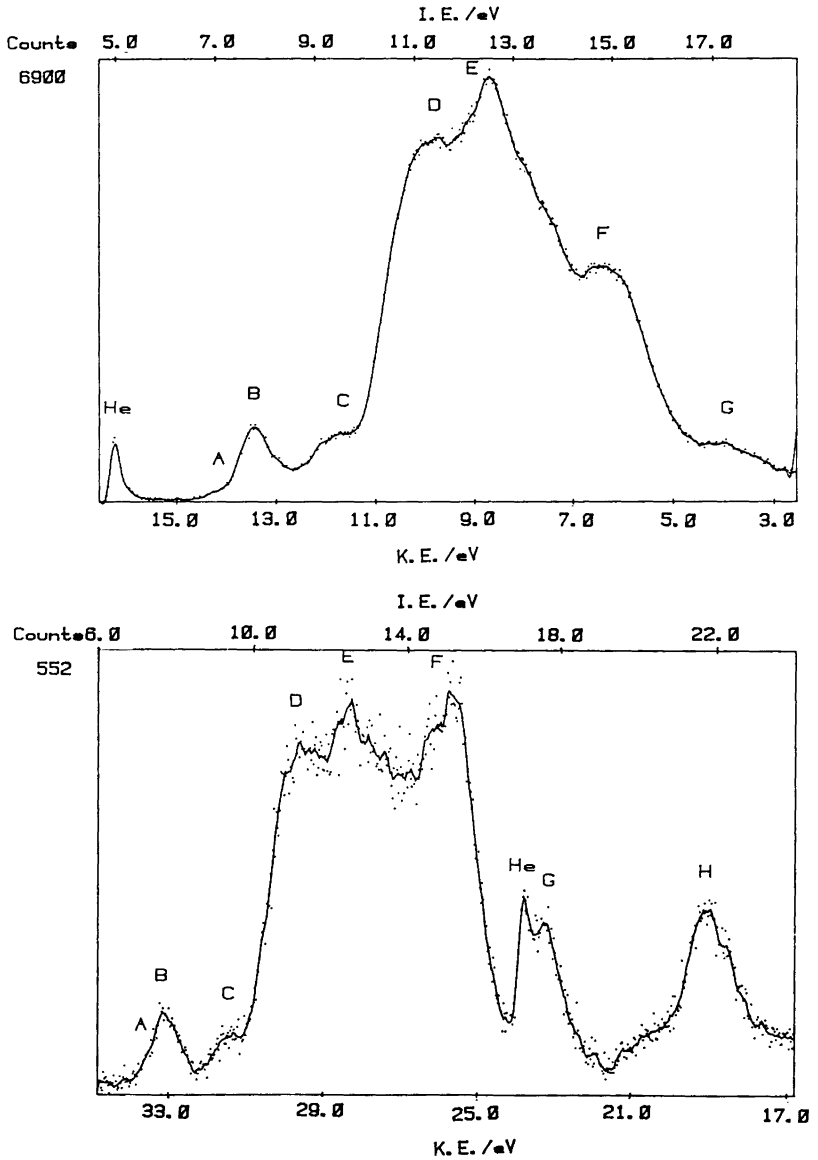

Fig. 4. He I and He II photoelectron spectra of $Mn(CH_2CMe_3)_2$ (= $Mnnp_2$).

Least-squares refinements were based on a model in which the valence angle $\angle MnC^iH^i$ was fixed at 106°, which yielded a calculated $Mn\cdots H^i$ distance of 253 pm. If $\angle MnC^iH^i$ is reduced to 75°, $Mn\cdots H^i$ is reduced to 220 pm, still significantly longer than the agostic interaction in $Mn(\eta\text{-}C_6H_8Me)(CO)_3$, where $Mn\cdots H$ = 184(1) pm.[16]

The molecular structure of CrR_3 has been determined by X-ray crystallography.[17] In this compound $\angle SiC^iSi$ = 118.2(6)°, and the small value compared to MnR_2 may be partly due to interligand repulsion. The difference between the Cr–C and Mn–C bond distances [Cr–C = 207(1) pm[17] and Mn–C = 201(3) pm] is of the magnitude expected for neighbouring 3*d* elements.

When comparing the Mn–C bond distances in

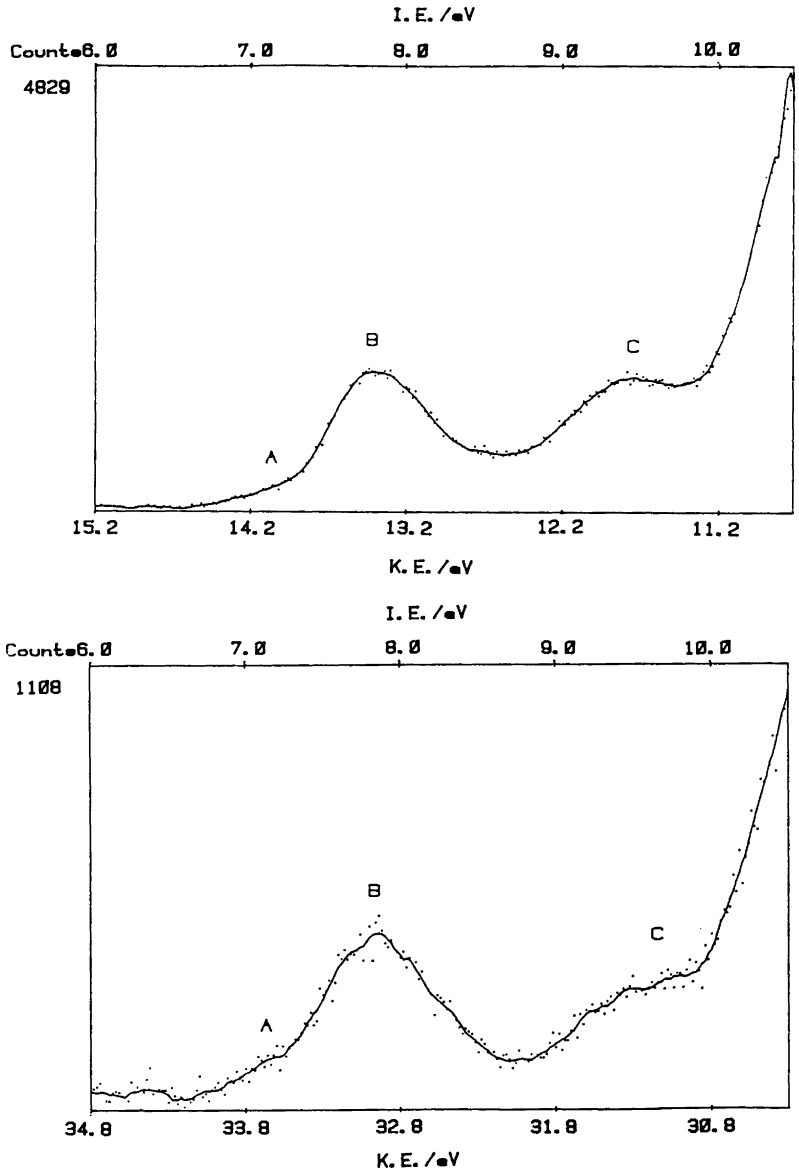

Fig. 5. Low ionization energy regions of the spectra shown in Fig. 4.

MnR_2, $Mnnp_2$ and $Mn\{C(Si–Me_3)_3\}_2$ it should be kept in mind that the Mn–C root-mean-square amplitudes of vibration obtained in the GED studies of the first two, l(Mn–C) = 10(4) pm (R) and 9.2(12) pm (*np*), indicate that the bond is easily deformed: The Mn–C stretch force constant obtained from the *ab initio* calculations on $MnMe_2$ (see below) indicates that the energy required to increase the length by 9 pm is only about 8 kJ mol^{-1}. We believe the greater Mn–C bond distance in $Mn\{C(SiMe_3)_3\}_2$ to be at least partly due to inter-ligand repulsion.[4] In this molecule $\angle SiC^iSi$ = 112.3(2)°, significantly smaller than in $HC^i(SiMe_3)_3$,[18] where $\angle SiC^iSi$ = 116.3(8)°.

The longer Mn–C bond distance in $Mnnp_2$ may, again at least in part, be an electronic effect; the Group 4 metals Ti and Zr are known to form significantly weaker bonds to CH_2CMe_3 than to CH_2SiMe_3.[19]

We now turn our attention to the results of MO calculations on $Mn(CH_3)_2$ and the photoelectron spectra of $Mnnp_2$. While these studies fail to throw light on the Mn–C bond distance differences discussed above, they do provide general information on metal-carbon bonding in Mn(II) alkyls.

Since permutation of the five electrons between the 3*d* orbitals yield only one $^6A_1$ state, *high-spin* $Mn(CH_3)_2$ is expected to be adequately described within the Hartree-Fock approximation. *Ab initio* MO calculations yield an optimal Mn–C bond distance of 213 pm, in good agreement with the bond distances in $Mn\{C(SiMe_3)_3\}_2$ and $Mnnp_2$, and 6% greater than in MnR_2. The energies of the highest occupied MO's and some population parameters are listed in Table 3. The net atomic charge on Mn appears to be quite high (+1.40), as expected for *high-spin* Mn(II); the net charge on Zn obtained in similar calculations on $Zn(CH_3)_2$[20] is +0.92. Sine the population of each $3d\pi$ orbital on Mn is 1.00, there appears to be no back-donation of C–H bond pairs into these orbitals. The population of the $3d\sigma = 3d_z^2$ orbital is 1.11, indicating some interaction with the Mn–C σ-bonding system.

The photoelectron spectra of $Mnnp_2$ are shown in Figs. 4 and 5. The points give the experimental data, the solid lines represent least-squares fits to these points.

In the region above 10 eV (Fig. 4) the spectral profile is characteristic of the *neo*pentyl ligand and may be compared to that found for *neo*pentane itself[21] or $Crnp_4$.[22] The resemblance is most pronounced in the He II spectrum, indicating that in the He I spectrum we are losing intensity from the slow electron bands, presumably as a result of contamination of the target chamber and analyzer during the course of the run.

In the region below 10 eV (Fig. 5), three distinct ionization features are visible though the first (A) is weaker than the other two (B and C). A is, however, not of the correct kinetic energy or intensity to be a shadow of the main band caused by additional lines in the discharge source, and its position in the spectrum is consistent between the He I and He II regions. Its intensity is greater in the He II spectrum, indicating that it may be part of the 3*d* band manifold.

In the PE spectrum of $Crnp_4$ a band at 7.25 eV has been assigned to 3*d* ionization while a peak at 8.37 eV has been assigned to ionization from the t_{2g} Cr–C bonding orbital. $Mn(\eta–C_5H_5)_2$, a pseudo-linear *high-spin* Mn(II) compound, has PE bands assigned to *d* ionizations at 6.91, 10.10 and 10.51 eV.[23] These *d* bands are broad, as ionization of *d* electrons in *high-spin* molecules is associated with significant changes in metal-ligand bond lengths; similar broad bands are commonly found for ionization of *f*-bands in lanthanide and actinide compounds (see for example Ref. 24). We consequently assign band A to ionization from the $3d\sigma$ orbital, which according to our calculations on $Mn(CH_3)_2$ and ligand field considerations should be the highest *d* orbital. Bands B and C are assigned to the highest occupied molecular orbitals of $Mn(CH_3)_2$, the asymmetric and symmetric Mn–C σ-bonding orbitals. Since ionization from the metal-centered $3d\sigma$ orbital is expected to be accompanied by greater relaxation of the molecular ion, it is not unexpected that it will require less energy than indicated by orbital energy considerations.

Acknowledgements. We dedicate this article to Professor Otto Bastiansen who helped us launch structural studies of organometallic compounds in Oslo. The work in Berkeley was supported by The University of California Committee of Research and a postdoctoral fellowship for D.J.B. from NSERC (Canada), the work in Brighton and Oxford by the S.E.R.C., and the work in

Oslo by the Norwegian Research Council for Science and the Humanities.

References

1. Andersen, R. A., Carmona-Guzman, E., Gibson, J. F. and Wilkinson, G. *J. Chem. Soc., Dalton Trans.* (1976) 2204.
2. Snow, A. I. and Rundle, R. E. *Acta Crystallogr. 4* (1951) 348.
3. Gambarotta, S., Floriani, C., Chiesi-Villa, A. and Guastini, C. *J. Chem. Soc., Chem. Commun.* (1983) 1128.
4. Buttrus, N. H., Eaborn, C., Hitchcock, P. B., Smith, J. D. and Sullivan, A. C. *J. Chem. Soc. Commun.* (1985) 1380.
5. Andersen, R. A., Haaland, A., Rypdal, K. and Volden, H. V. *J. Chem. Soc. Chem. Commun.* (1985) 1807.
6. Evans, D. F. *J. Chem. Soc.* (1959) 2003.
7. Davidson, P. J., Harris, D. H. and Lappert, M. F. *J. Chem. Soc., Dalton Trans.* (1976) 2268.
8. Schäfer, L., Yates, A. C. and Bonham, R. A. *J. Chem. Phys. 55* (1971) 3055.
9. Almløf, J., Fægri, K., Jr. and Korsell, K. *J. Comput. Chem. 3* (1982) 385.
10. Roos, B., Veillard, A. and Vinot, G. *Theor. Chim. Acta 20* (1971) 1.
11. Roos, B. and Siegbahn, P. *Theor. Chim. Acta 17* (1970) 209.
12. Duijneveldt, F. B. *IBM Technical Research Report No. RJ-945* (1971).
13. Fjeldberg, T., Seip, R., Lappert, M. F. and Thorne, A. J. *J. Mol. Struct. 99* (1983) 295.
14. Fjeldberg, T., Haaland, A., Schilling, B. E. R., Lappert, M. F. and Thorne, A. J. *J. Chem. Soc. Dalton Trans.* (1986) 1551.
15. Brookhart, M. and Green, M. L. H. *J. Organomet. Chem. 250* (1983) 395.
16. Schultz, A. J., Teller, R. G., Beno, M. A., Williams, J. M., Brookhart, M., Lamanna, W. and Humphrey, M. B. *Science 220* (1983) 197.
17. Barker, G. K., Lappert, M. F. and Howard, J. A. K. *J. Chem. Soc., Dalton Trans.* (1978) 734.
18. Beagley, B. and Pritchard, R. G. *J. Mol. Struct. 84* (1982) 129.
19. Lappert, M. F., Patil, D. S. and Pedley, J. B. *J. Chem. Soc., Chem. Commun.* (1975) 830.
20. Almenningen, A., Helgaker, T. U., Haaland, A. and Samdal, S. *Acta Chem. Scand. Ser., A 36* (1982) 159.
21. Evans, S., Green, J. C., Joachim., P. J., Orchard, D. W., Turner, D. W. and Maier, J. P. *J. Chem. Soc., Faraday Trans. 2, 68* (1972) 905.
22. Evans, S., Green, J. C. and Jackson, S. E. *J. Chem. Soc., Faraday Trans. 2, 69* (1973) 191.
23. (a) Evans, S., Green, M. L. H., Jewitt, B., King, G. H. and Orchard, A. F. *J. Chem. Soc., Faraday Trans. 2, 70* (1974) 356; (b) Rabalais, J. W., Werme, L. O., Bergmark, T., Karlsson, L., Hussain, M. and Siegbahn, K. *J. Chem. Phys. 57* (1972) 1185; (c) Cauletti, C., Green, J. C., Kelly, M. R., Powell, P., van Tilborg, J., Robbins, J. and Smart, J. *J. Electron Spectrosc. Relat. Phenom. 19* (1980) 327.
24. Green, J. C., Payne, M., Seddon, E. A. and Andersen, R. A. *J. Chem. Soc., Dalton Trans.* (1982) 887.

Received February 16, 1988.